

Triple-point wetting of multilayer films physisorbed on graphite

G. Zimmerli* and M. H. W. Chan

Department of Physics, Pennsylvania State University, University Park, Pennsylvania 16802

(Received 9 August 1990; revised manuscript received 16 December 1991)

A graphite fiber microbalance technique is used to study the growth mode of Kr, Xe, CH₄, and CO films on graphite. The maximum thickness of the adsorbed film is finite below the triple points T_i of each of these adsorbates. The maximum thickness increases rapidly as T is brought toward T_i and levels off for $T \geq T_i$. This behavior is suggestive of a wetting transition that is pinned at the respective T_i of adsorbates.

INTRODUCTION

The study of a film physisorbed on a smooth substrate provides a convenient way to investigate the crossover from two-dimensional to three-dimensional behavior. To do so, one must be able to vary continuously the thickness of the adsorbed film from the monolayer to macroscopically thick multilayers by, for example, simply increasing the equilibrium vapor pressure of the adsorbate. When this is possible, the adsorbate is said to completely wet the substrate. The actual maximum film thickness is often limited by gravitational and other thinning effects to tens of layers. Another distinct possibility for the evolution of the film is that increasing the vapor pressure of the adsorbate towards the saturated vapor pressure results in no additional adsorption in the film phase. In this case the adsorbed film coexists, in equilibrium, with three-dimensional (3D) bulk at saturation and the adsorbate is said to wet the substrate incompletely. A wetting transition occurs when the adsorbate-substrate system undergoes a transition from incomplete wetting to complete wetting at some temperature T_w .

A recent lattice-gas treatment of multilayer adsorption suggests that the relative strengths of adsorbate-adsorbate and adsorbate-substrate attractions determine the wetting nature of a particular system.¹ Complete wetting is expected at low temperatures if adsorbate-substrate attractions dominate (strong substrate) over weaker adsorbate-adsorbate attractions. Incomplete wetting is expected for weak substrates. For substrates of intermediate strength a wetting transition at T_w is possible. However, experimental studies found incomplete wetting growth for a number of solid films with strong adsorbate-substrate interactions.² This discrepancy has been explained to be related to the strain induced by structural mismatch between successive solid layers, which prevents complete wetting by a solid phase.³ In such a scenario, one would expect, for a system of strong adsorbate-substrate interaction, the pinning of the wetting transition at the triple point T_i of the adsorbate to be a general phenomenon.⁴ Indeed, triple-point wetting transitions have been reported in a number of systems, e.g., O₂ on graphite,^{5,6} Ne and H₂ on Ag,⁷ and a number of adsorbates on Au.⁸ On the other hand, this expectation is not consistent with the widely accepted interpreta-

tion of classic volumetric vapor pressure isotherm experiments^{9,10} that Ar, Kr, Xe, and CH₄ wet graphite at temperatures well below their triple points. Since incomplete wetting at low temperatures is found for systems that have adsorbate-substrate interactions both stronger and weaker¹¹ than these four adsorbates, these four adsorption systems are described as exhibiting reentrant wetting growth.²

A recent adsorption study of Ar on graphite, however, performed with the graphite fiber microbalance technique, found results indicative of incomplete wetting at low temperature.¹² The maximum thickness of the adsorbed Ar film is found to be limited to five layers at low temperatures, with no evidence of continued film growth as pressure is brought towards P_0 . However, the limiting film thickness at $P = P_0$ is found to diverge as the temperature of the isotherm is brought towards the triple point T_i of Ar.

The vast amount of experimental work of multilayer noble and van der Waals molecules adsorbed on graphite has recently been reviewed by Hess.¹³ In addition to complete and incomplete wetting growth, experimental evidence of surface melting, surface roughing, interface-induced freezing, and layer critical points of a multilayer film are also discussed by Hess. In this paper we shall examine in some detail the evidence for the reentrant wetting growth of these four adsorption systems and present our multilayer adsorption isotherm results of Xe, Kr, CH₄, and CO on graphite utilizing the graphite fiber microbalance technique. CO on graphite is interesting because the result of a recent volumetric isotherm study¹⁴ was interpreted to be indicative of a wetting transition pinned at the orientational transition of the α and β phases of bulk solid CO. CH₄ on graphite is interesting because the result of a series of heat capacity¹⁵ and NMR experiments¹⁶ with exfoliated graphite was interpreted to go through a sequence of wetting, dewetting, and wetting transitions as the temperature is brought toward the triple point from below. We also present an adsorption study of CF₄ on graphite, showing the capability of the fiber technique in detecting incomplete wetting growth. CF₄ on graphite is the most clearcut nonwetting system, since adsorbed film is limited to only two layers below 72 K. Our results of Xe, Kr, CH₄, and CO on graphite are consistent with the finding of the Ar on graphite fiber ex-

periment and appear to support the simple picture of a wetting transition pinned at the bulk triple point of these adsorbates.⁴

EXPERIMENTAL APPARATUS

The experimental setup of this study is similar to that used previously by Bartosh and Gregory⁵ to study the growth mode of O₂ on graphite. It is also similar to that used by Taborek and Senator¹⁷ and by us¹⁸ to investigate the wetting properties of liquid helium on graphite. It differs from the arrangement used by Bruschi, Torzo, and Chan¹² in that excitation of the fiber is achieved by electrical rather than mechanical means.

This experiment utilizes P-130 graphite fibers supplied by Amoco Performance Products.¹⁹ These fibers are of a higher quality than the P-120 and P-100 fibers used in the O₂,⁵ He,^{17,18} and Ar (Ref. 12) experiments. The electrical and thermal conductivity of P-130 fibers are nearly a factor of 2 greater than that of P-120 fibers and only a factor of 3 smaller than that of single-crystal graphite. Electron microscopy pictures, taken by us and others, show that the basal planes are oriented as long and narrow facets that run parallel to the fiber axis. Imperfections appear in the form of ridge-trough structures,¹⁸ also along the fiber axis. The separation of the ridge-trough imperfections are found to be on the order of 1000 Å. The P-130 fiber has also been used recently to study the adsorption of Ar.²⁰ The sharpness of the second step in this study indicates the surface single-crystal basal plane domains have characteristic lengths of 200 Å. In our experiment, a single fiber, ~10 μm in diameter and 1 cm long, is mounted to a sample holder containing a small permanent magnet and pole pieces. One end of the fiber is attached to a rigid support with silver epoxy. The other end is attached, also with silver epoxy, to a cantilever spring made from 0.002-in.-thick Be-Cu foil that maintains a nearly constant tension in the fiber upon changes in temperature of the holder. The sample mount is placed inside a copper sample cell that is temperature regulated to better than 1 mK. Cleaning of the fiber surface is done *in situ* before each isotherm by simply passing 15–20 mA of current through the fiber, heating it to an average temperature of 400°C.

A small ac current (~0.1–1 μA) of frequency f_0 is used to excite the fundamental mode of vibration. The fiber vibrates perpendicular to the magnetic field, and the amplitude of vibration is kept sufficiently small ($\ll 1 \mu\text{m}$) such that we observe no dependence of f_0 on the driving current. In vacuum, the resonant frequency f_0 is given by²¹

$$f_0 = \frac{1}{2l} \left[\frac{T}{\rho_w S} \right]^{1/2} \left[1 + \frac{r}{l} \left[\frac{YS}{T} \right]^{1/2} \right], \quad (1)$$

where T is the tension, l is the length, ρ_w is the fiber density (2.18 g/cm³), r is the radius, S is the cross-sectional area, and Y is Young's modulus (7×10^{12} dyn/cm²). The second term in brackets represents the contribution from the natural stiffness of the fiber. Equation (1) is valid as long as the tension is the dominant restoring force. At our operating frequency of 21 kHz this is indeed the case.

ADSORPTION AND HYDRODYNAMIC EFFECTS

The shift in resonant frequency Δf from the adsorption of a film of thickness d and density ρ_l is

$$\frac{\Delta f}{f} = - \frac{d \rho_l}{r \rho_w}. \quad (2)$$

The vapor surrounding the oscillating fiber also causes the resonant frequency to change due to the effect of viscous drag. Stokes was the first to work out the hydrodynamics of a cylinder oscillating in a fluid.²² The result is that the resonant frequency ν of a wire surrounded by a vapor of density ρ_v is given by

$$\nu = \nu_0 \left[\frac{\rho_w}{\rho_w + k \rho_v} \right]^{1/2}, \quad (3)$$

where ν_0 is the vacuum resonant frequency, ρ_w is the wire density, and k is the Stokes function. This coefficient k is a function of the dimensionless parameter q given by

$$q = \frac{r}{2} \left[\frac{2\pi f \rho_v}{\eta} \right]^{1/2} = \frac{r}{2\lambda}, \quad (4)$$

where η is the viscosity of the vapor and λ is the viscous penetration depth. Values of k versus q are tabulated in Stokes's paper.

In order to determine the frequency shift Δf due to the adsorption of a film, the hydrodynamic effect as shown in Eq. (3) must be subtracted properly. In the absence of adsorption, the resonant frequency of the fiber as a function of pressure should be described by Eq. (3). Figure 1 shows isotherm data for Kr at 293 K along with the Stokes-theory prediction for two different values of the fiber radius. A value of $r = 4.8 \mu\text{m}$ gives the best fit to the data and will thus be used for quantitative analysis for this paper.

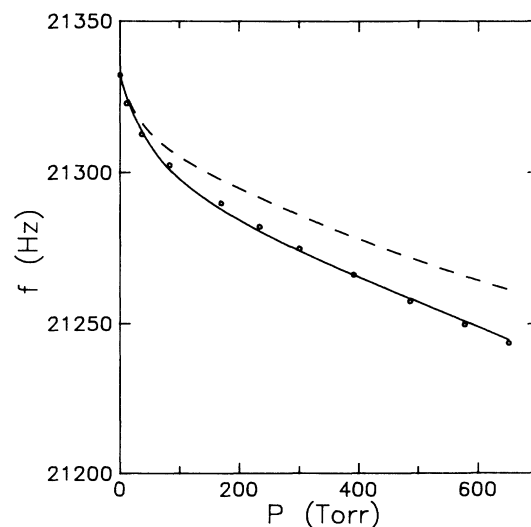


FIG. 1. Resonant frequency as a function of pressure for Kr near room temperature. The calculated hydrodynamic background is shown for two different values of the fiber radius: dashed line, $r = 6.0 \mu\text{m}$; solid line, $r = 4.8 \mu\text{m}$.

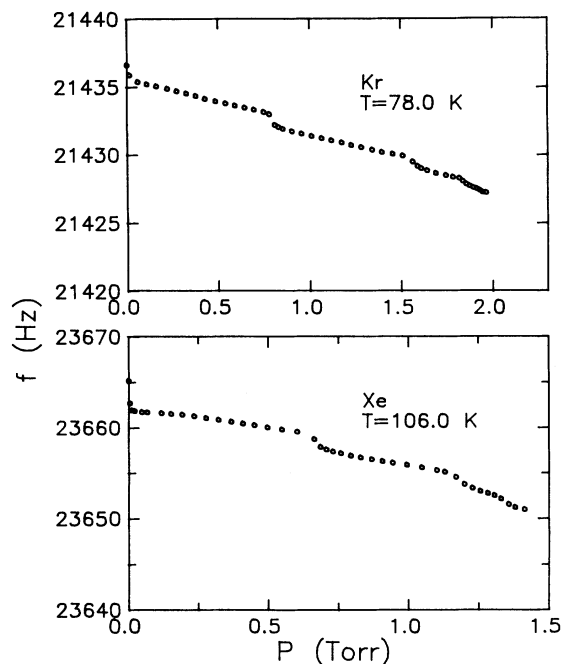


FIG. 2. Resonant frequency as a function of pressure for Kr and Xe. Both isotherms display stepwise growth of at least four layers.

EXPERIMENTAL RESULTS

Isotherms of Xe at 106.0 K and Kr at 78.0 K are shown in Fig. 2. The resonant frequency of the fiber is plotted versus pressure up to the bulk saturated vapor pressure P_0 . Four steps, at P/P_0 values consistent with volumetric adsorption isotherms⁹ studies using exfoliated graphite substrates, can be clearly resolved. The resonant frequency shows very little additional decrease beyond the fourth step. This finite frequency drop indicates that the small bulk crystallites that form in the $P=P_0$ limit do not stick to the graphite fiber. A possible explanation for nonsticking is that the equilibrium size of the crystallites is substantially larger than the width (~ 1000 Å) of the long flat facets on the fiber surface.

In addition to frequency shifts due to layer condensations, the isotherms also display a smooth background related to hydrodynamic damping. The first step is partially masked by the initial rapid drop in frequency due to this effect. The equations of hydrodynamics are only strictly valid when the mean free path of the atoms or molecules in the vapor is much smaller than the radius of the fiber. For the isotherms in Fig. 2, the mean free path is always more than twice the diameter of the fiber, and so we are unable to apply the Stokes theory in this case. Whenever applicable, we will show the hydrodynamic background as calculated from Eq. (3). As the pressure of the sample chamber is increased towards P_0 , the resonant frequency of the fiber actually increases slightly. This phenomenon is seen for isotherms taken at temperature substantially below the triple point of the adsorbate. This phenomenon has also been reported in an earlier

graphite fiber experiment.⁵ For Xe and Kr, this positive shift is typically a few Hz above the minimum value. We have investigated this effect by repeating isotherms near and below 110 K with the same as well as with different graphite fibers. Whereas the pressure of the layering steps is always reproducible, the magnitude of the positive shift at P_0 varies from run to run. This positive shift diminishes with temperatures and becomes unobservable when the temperature of the sample chamber is brought to within a few degrees below the triple point of the adsorbate. One possible explanation of the positive shift is that the thickening solid film is contributing to the stiffness term in Eq. (1).⁵ This is unlikely to be correct, since we have seen that the layering of the first four solid layers causes the frequency to decrease. Furthermore, the additional stiffening of a solid film of a few layers is expected to be minute compared to that of the fiber at 4.8 μm in radius. The most reasonable explanation is that near P_0 at low temperatures, small solid crystallites are nucleating from the two ends of the fiber where it is attached to the silver epoxy patches. The observed positive-frequency shift can be accounted for by a decrease of one micrometer in the effective length of the fiber. Under the microscope, the silver epoxy are found not to wet the fiber, and the joints are formed with the epoxy drying around and clamping the fiber. We speculate that the crevices between the fiber and the epoxy patches are the likely nucleation centers of the solid crystallites. As temperature is brought towards T_t , this effect vanishes, perhaps because the small solid crystallites undergo surface melting for T near T_t .

The important conclusion to be drawn from the data in Fig. 2 is that the film growth of Kr and Xe and graphite, as was found for Ar on graphite,^{12,20} is limited to a few layers at temperatures far below the respective triple points. This is indicative of incomplete wetting. As a comparison, isotherms of Kr and Xe performed at temperatures just below and above the respective triple points, are shown in Figs. 3 and 4. The isotherms taken just above the respective triple points show a divergent drop in the frequency as P is brought towards P_0 . The total drop in frequency is limited for isotherms taken below their triple points. The magnitude of the total decrease in frequency diminishes rapidly as the temperature of the isotherm is reduced from T_t . Since the layer critical points of the second and higher layers are well below the triple points of the various adsorbates,¹³ the isotherms shown in Figs. 3 and 4, in contrast to those shown in Fig. 2, do not show a stepwise decrease in the frequency. The magnitude of the hydrodynamic background also increases at higher temperatures due to the corresponding increase in vapor density and viscosity. The dashed line indicates the hydrodynamic contribution to the frequency shift as calculated from Eq. (3). Values for the vapor viscosity were taken from Ref. 23. The vapor density was calculated from the equation of state including second virial coefficients.²⁴ After subtraction of the hydrodynamic contribution, the total decrease in frequency at $P=P_0$ shown in Figs. 3 and 4 translates through Eq. (2) to an effective film thickness of 13 layers for Kr and 17 layers for Xe at temperatures 2.8 and 0.8 K

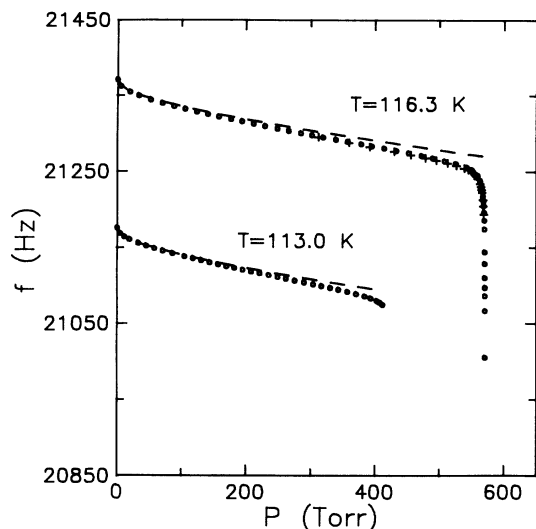


FIG. 3. Resonant frequency as a function of pressure for isotherms of Kr above and below the triple-point temperature ($T_i = 115.8$ K). The dashed line indicates the hydrodynamic background as calculated from the Stokes theory. The 113.0-K ($P_0 = 413$ Torr) isotherm has been shifted down by 200 Hz for clarity. The circles and crosses of the 116.3-K isotherm ($P_0 = 570.5$ Torr) are adsorption and desorption data, respectively.

below their respective triple points. The maximum thickness for isotherms taken 0.5 K (Kr) and 0.3 K (Xe) above the triple points is on the order of 100 layers. The most straightforward interpretation of Figs. 3 and 4, as stated in the Introduction, is that Xe and Kr on graphite exhibit triple-point wetting.

The isotherm of Kr above the triple point in Fig. 3 also

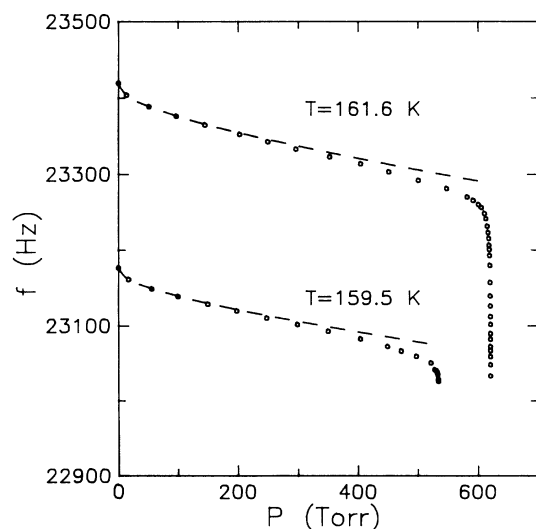


FIG. 4. Resonant frequency as a function of pressure for isotherms of Xe above and below the triple point ($T_i = 161.3$ K). The dashed line indicates the calculated hydrodynamic background. The 159.5-K isotherm ($P_0 = 534.2$ Torr) has been shifted down by 240 Hz. $P_0 = 620.5$ Torr at 161.6 K.

shows desorption data. After completing the adsorption isotherm, small doses of gas were removed and the resonant frequency was measured as a function of decreasing pressure. We found no evidence of a hysteresis loop in the adsorption-desorption cycle, in contrast to volumetric vapor-pressure isotherm studies using exfoliated graphite substrates.

As shown in Figs. 5 and 6, the isotherm results for CH_4 and CO are similar to those of Kr and Xe. Because CH_4 and CO have much smaller molecular weights than Kr and Xe, the frequency shifts due to adsorption and hydrodynamic background are also smaller. The fact that the calculated hydrodynamic curve for CH_4 falls below the measured isotherm is an unphysical artifact. This is very likely a result of the combined uncertainties in both the resonant-frequency measurements (discussed below) and the calculated hydrodynamic correction. In contrast to the interpretation of Ref. 14, our data on CO show a continuous increase in film thickness as the temperature is raised through the bulk solid α - β transition at 61.5 K. A "divergent" increase in the film thickness is found, however, as T is brought towards the triple point at 68.1 K. A very recent ellipsometry experiment reached similar conclusions regarding the growth mode of N_2 on graphite. Namely, there is incomplete wetting growth both below and above the α - β transition and the wetting transition is likely to be pinned at the solid-liquid-vapor triple point.²⁵ Considering the similarity of the bulk and monolayer phases, the similarity in the growth modes of CO and N_2 on graphite is expected.

The results of the various isotherms are summarized in Fig. 7. Here we have plotted Δf , the maximum frequency shift due to mass loading of the adsorbed film at $P = P_0$, as a function of temperature for the adsorbates Kr, Xe, CO, and CH_4 . In each case, the total drop in fre-

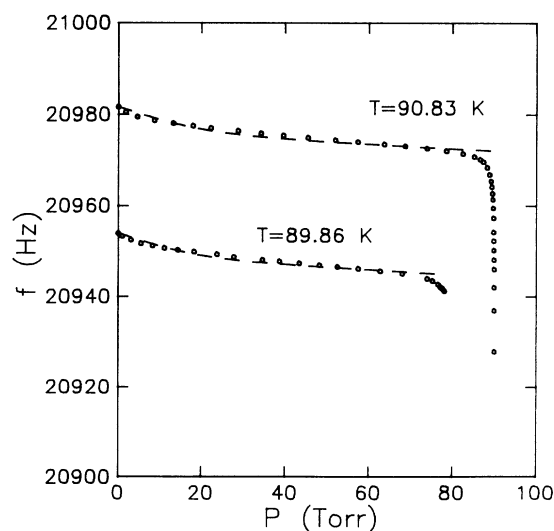


FIG. 5. Resonant frequency as a function of pressure for isotherms of CH_4 above and below the triple point ($T_i = 90.66$ K). The dashed line indicates the calculated hydrodynamic background. The 89.86-K isotherm ($P_0 = 78.32$ Torr) has been shifted down by 30 Hz. $P_0 = 89.96$ Torr at 90.83 K.

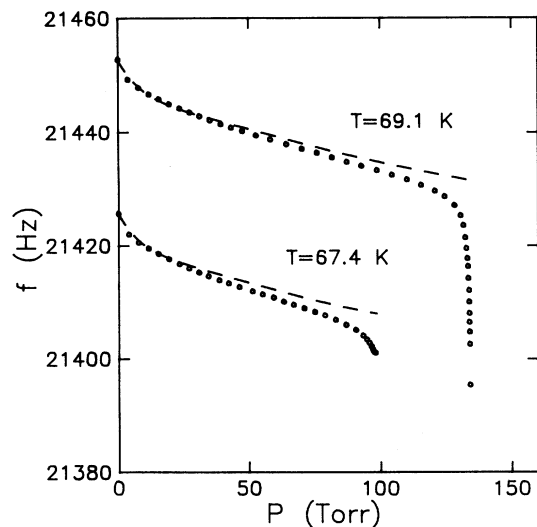


FIG. 6. Resonant frequency as a function of pressure for isotherm of CO above and below the triple point ($T_t = 68.1$ K). The dashed line indicates the calculated hydrodynamic background. The 67.4-K isotherm ($P_0 = 98.56$ Torr) has been shifted down by 30 Hz. $P_0 = 134$ Torr at 69.1 K.

quency and hence the maximum film thickness exhibit a rapid but continuous increase as T is brought toward T_t and levels off for $T \geq T_t$. This result is suggestive of a wetting transition that is pinned at the respective bulk triple point of the adsorbate. We shall comment on the discrepancies that exist in the literature after a discussion of the experimental results.

ANALYSIS AND DISCUSSION OF GRAPHITE FIBER RESULTS

When an adsorbate wets a flat substrate, the film thickness d can be compared with the Frenkel-Halsey-Hill (FHH) relation²⁶

$$d = \left[\frac{T}{\gamma} \ln \left(\frac{P_0}{P} \right) \right]^x, \quad (5)$$

where γ characterizes the strength of the adsorbate-substrate interaction and the exponent $x = -\frac{1}{3}$ reflects the nature of the van der Waals attraction. The FHH relation can be considered to be an approximation of the Dzyaloshinskii, Lifshitz, and Pitaevskii (DLP) theory,²⁷ omitting retardation and many-body effects.²⁸ In order to compare the measured frequency shift Δf due to mass

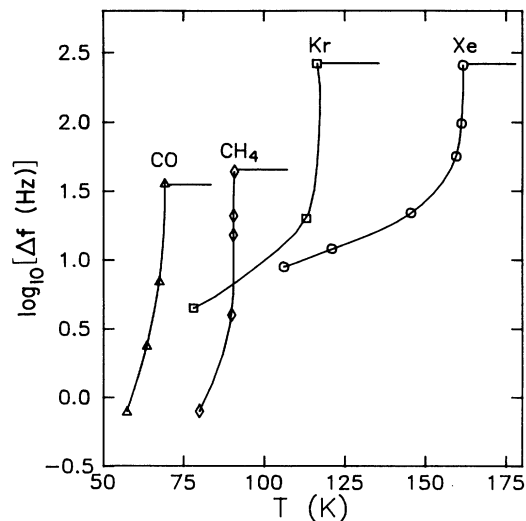


FIG. 7. The frequency shift due to the film as a function of temperature for the adsorbates used in this study. The "divergence" near the triple point in each case is indicative of triple-point wetting. The solid lines are drawn as a guide to the eye.

loading with the FHH relation as shown in Eq. (5), the frequency shift due to hydrodynamic damping must be subtracted properly. There are three major sources of error that limit the accuracy in determining Δf .

One potential source of error lies in the uncertainty of the hydrodynamic contribution to the total frequency shift. As can be seen from Eq. (4), the hydrodynamic background is sensitive to the choice of fiber radius, and the viscosity and density of the adsorbate vapor. The sensitivity to r is shown in Fig. 1. The viscosity of the various adsorbate gases is typically known to within only 10%. As stated previously, the equations of hydrodynamics are only strictly valid when the mean free path of the atoms or molecules in the vapor is much less than the fiber radius. In calculating the mean free path, we use the following expression:²⁹

$$l_{\text{MFP}} = \frac{\eta}{0.499\rho_v} \left(\frac{\pi M}{8RT} \right)^{1/2}, \quad (6)$$

where R is the gas constant and M is the molecular weight. In Table I we show the value of l_{MFP}/r at the P_0 for the different isotherms, and it can be seen that in most cases we have $l_{\text{MFP}} < r/100$. Table I also shows other parameters relevant to the present discussion.

A second source of error in our measurements of Δf

TABLE I. Values of parameters used in analyzing data near the triple point. Values for γ are taken from Ref. 32. For lack of a better value, we use the same γ value for CO as that given for N_2 .

Adsorbate	γ ($\text{K} \text{ \AA}^3$)	η (μP)	ρ_l (g/cm^3)	l_{MFP}/r	$\Delta f' + \Delta f''$ (Hz)
CO	10 300	46.6	0.85	7.7×10^{-3}	± 1.0
CH_4	12 400	37.5	0.45	1.4×10^{-2}	± 0.6
Kr	12 000	105.8	2.45	3.1×10^{-3}	± 3.3
Xe	16 200	130.6	2.98	3.3×10^{-3}	± 4.4

resides in the absolute determination of the resonant frequency. In our experimental setup, the graphite fiber is an element in an ac Wheatstone bridge circuit that is balanced to a null away from the resonant condition. When the bridge is driven at the resonant frequency f , an induced voltage (typically $\sim 5 \mu\text{V}$) $V_0 = V_F + iV_q$ results from the oscillation of the fiber in the magnetic field. The quadrature component V_q is used to form a phase-locked feedback loop to drive the voltage-controlled oscillator in at the resonant frequency. The proper phase of the oscillator is set by maximizing the induced signal V_0 .

Any error in the phase setting ϕ will lead to an error $\Delta f'$ in the measurement of the resonance frequency given by³⁰

$$\Delta f' = f \tan \phi / 2Q, \quad (7)$$

where Q is the quality factor of the oscillator. Given a signal-to-noise ratio of 10^3 at the output of the lock in, our method for setting the phase can result in a phase error of $\pm 2^\circ$. The quality factor due to the hydrodynamic drag can be evaluated from the Stokes theory²² and is given by

$$Q = \frac{\rho_w}{\rho_v k'}, \quad (8)$$

where k' is again a function of the parameter q defined in Eq. (4). Taking Xe near the saturated vapor pressure as an example, we have from Eq. (8) $Q = 140$, so that a phase error of $\pm 2^\circ$ would result in an error in the measured resonant frequency of $\Delta f' = \pm 2.8$ Hz.

A third source of error in the resonant-frequency measurement is due to residual signals that cannot be completely nulled out. If the residual voltage V_R is in phase with V_q , then an additional error $\Delta f''$ is introduced:³⁰

$$\Delta f'' = f \frac{V_R}{V_0} \frac{1}{2Q}. \quad (9)$$

A typical value might be $V_R/V_0 = \pm 1/50$, so that for Xe where $Q = 140$ we would have $\Delta f'' = \pm 1.6$ Hz. In our example for Xe, the combined effect of Eqs. (7) and (9) is such that it results in an uncertainty in Δf of ± 4.4 Hz near the saturated vapor pressure. A similar analysis for the other adsorbates leads to the expected uncertainties listed in Table I.

An uncertainty in Δf of 4 Hz for Xe near saturated vapor pressure corresponds to a relative uncertainty of slightly more than 1%. The uncertainty is smaller at low pressure, since the Q of the vibrating fiber is higher.

The measured frequency shift due to mass loading of the low-temperature isotherm Δf_{expt} as shown in Fig. 2, is found to be consistent with the expected values. For example, if we apply Eq. (2) to the case of Xe, we would expect a frequency decrease of 2.8 Hz/layer, and a total decrease of 11.2 Hz is expected for a four-layer film. A total shift of 14 Hz is found. The agreement becomes better if we allow for hydrodynamic corrections.

The quantitative dependence of Δf_{expt} on P/P_0 for isotherms taken above T_i is not consistent with the Frenkel-Halsey-Hill relation. According to Eqs. (2) and

(5), a plot of $\log_{10}(\Delta f)$ versus $\log_{10}(\ln P_0/P)$ of these isotherms should yield a slope of $-\frac{1}{3}$. This is not found in any one of the four adsorption systems. For Kr and Xe, a slope of 0.42 ± 0.02 is found between $P/P_0 = 0.9$ and 0.9995. The measured frequency shifts Δf_{expt} near P_0 are found to be substantially larger than the calculated FHH value Δf_{calc} , with $x = -\frac{1}{3}$. The $\Delta f_{\text{expt}}/\Delta f_{\text{calc}}$ ratios for both Kr and Xe are found to be near unity at $P/P_0 = 0.5$, but increase rapidly to 2.4 at $P/P_0 = 0.9$, 3.0 at $P/P_0 = 0.99$, and 3.63 at $P/P_0 = 0.999$. A similar trend is found for CH_4 and CO. Such an enhancement in the effective liquid-film thickness in the limit of $P = P_0$ is also found in the graphite fiber experiment of ^4He ,¹⁸ Ar,^{12,20} and a number of other adsorbates.³¹ We think the enhanced adsorption as P approaches P_0 is related to the ridge-trough imperfections on the surface of the graphite fiber.

The profile of an adsorbed liquid film adsorbed near a wedge formed by two intersecting planes has been calculated by Cheng and Cole.³² They found, perhaps not surprisingly, that the film thickens near the center of the wedge. This excess condensation becomes significant when the thickness of the film d in the flat region, i.e., far from the wedge, exceeds a characteristic length $\zeta = (nC_3/\sigma)^{1/2}$. C_3 , n , and σ are, respectively the constant describing the strength of the long-range van der Waals interaction, the number density and the surface tension of the film. For a noble gas, ζ is on the order of 5–10 Å. Indeed, they found the amount of "excess" increases as $(d/\zeta)^5 \cos \theta$, where 2θ is the angle of the wedge formed by the two flat planes. It should be noted that for $\theta > 90^\circ$, i.e., in the vicinity of a ridge, "thinning" of the adsorbed film is expected. However, the amount of thinning is limited by the attractive potential of the substrate. A simple estimate shows that excess adsorption as measured by $\Delta f_{\text{expt}}/\Delta f_{\text{calc}}$ near $P/P_0 = 0.9$ and 0.99 is qualitatively consistent with the model of Cheng and Cole. If we assume that the wedges on the surface of the fiber are separated from each other by 1000 Å, a wedge angle of 30° and a "true" film thickness d of ten layers (d is the thickness of the film far from the wedge), then the excess adsorption, according to Fig. 1 of Ref. 32, is three times the adsorbed film on a flat surface. It is difficult to make a more quantitative estimate of the expected excess adsorption, since wedges with a fixed angle are clearly not a realistic model of the ridge-trough imperfections on the surface of the fiber.

Figure 7 shows a rapid increase and then a leveling off of the maximum film thickness as T is brought toward and exceeds T_i . The fact that there is no discontinuous jump at $T = T_i$ suggests that the excess adsorption or film thickening also occurs for $T \lesssim T_i$. This is not surprising, since the top layers of the adsorbed film near and below T_i are expected and reported to be liquidlike, and hence favorable for excess adsorption. The smooth increase in the maximum thickness found as $T \rightarrow T_i$ is consistent with the prediction that the excess adsorption increases with d . (In the Cheng-Cole model, it scales as d^5 .) Although this excess adsorption prevents a quantitative comparison of our data with the FHH equation, we can-

not think of any mechanism that will mask the main, if only qualitative, observation of this experiment, namely the wetting transition that is pinned at the triple point of the adsorbate. The nonwetting growth mode at low temperature is unlikely to be an artifact of surface imperfections, since a rough surface tends to thicken and not reduce the film thickness.³³

The excess adsorption we found with the graphite fiber is qualitatively different from capillary condensation found in porous substrates such as exfoliated graphite. In particular, there is no sign of a hysteresis loop in the adsorption-desorption cycle. The difference is probably due to the fact that the "wedges" on the surface of the fiber are exposed and are in good contact with the vapor phase. In the case of porous substrates, the pores are separated by narrow openings.

In order to check the capability of our technique in distinguishing incomplete and complete wetting growth, we have made isotherm studies of CF_4 on graphite as a "control" experiment. We chose this system because there is a clean layering transition near 72 K. The fact that the molecular mass of CF_4 is comparable to Kr makes it convenient and relatively easy to detect the layering transition. In Fig. 8, isotherms at 90.6, 74.2, and 65.8 K are shown. Since the saturated vapor pressures of CF_4 at 74.2 and 65.8 K are very low (P_0 are 21 and 3 mTorr, respectively), we were not able to measure the pressure reliably; the resonant frequency of the fiber is measured as a function of the amount of CF_4 dosed into the sample chamber. The maximum frequency drop due to the adsorption of CF_4 is 3.3 Hz at 65.8 K and 5.33 Hz at 74.2

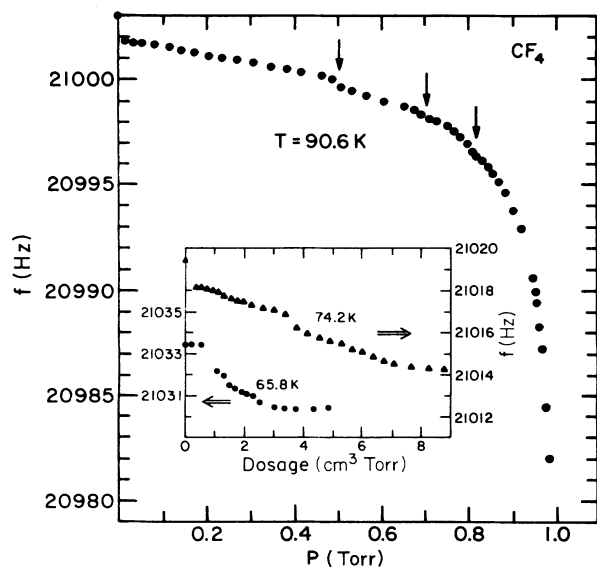


FIG. 8. Resonant frequency as a function of vapor pressure of CF_4 at 90.6 K ($P_0 = 1$ Torr). Stepwise growths of the second, third, and fourth layers are marked by arrows. The inset shows two isotherms measuring the resonant frequency as a function of total dosage of CF_4 . The total drop in frequency is consistent with an adsorbed film of maximum thickness of two (65.8 K) and three (74.2 K) layers.

K. These findings are consistent with the results of the recent heat-capacity³⁴ and ellipsometry³⁵ experiments indicating that below 72 K, the adsorbed film is limited to a thickness of two layers. There is a layering transition at 72 K, and above this temperature and up to 80 K, the maximum thickness of the adsorbed film is three layers, according to the heat-capacity study, and four layers according to the ellipsometry study. (The result shown in Fig. 8 appears to favor the heat-capacity result.) Upon further addition of CF_4 beyond the maximum dosage shown in the inset of Fig. 8, positive shifts in frequency are found. As discussed earlier, we think this positive shift is related to the nucleation of small crystallites at the ends of the graphite fiber.

The 90.6-K isotherm, taken above the triple point of CF_4 at 89.5 K, also indicates complete wetting growth consistent with other adsorbates. This isotherm is different from those shown in Figs. 3–6 in that stepwise growth of the second, third, and fourth layers can be identified. This is consistent with the ellipsometry findings³⁵ that the layer critical points of the first several layers of the CF_4 on graphite system are located above 100 K.

MULTILAYER ADSORPTION STUDIES USING EXFOLIATED GRAPHITE SUBSTRATE

The classic volumetric vapor-pressure isotherms of Xe, Kr, CH_4 , and Ar on exfoliated graphite substrate show layer-by-layer growth up to, at least four layers at low temperature.^{9,10} There is considerable ambiguity concerning the proper interpretation of the continuous increase in adsorption near $P = P_0$ beyond the layer-by-layer growth regime. Although such an increase is consistent with wetting growth (or conventional) interpretation, it can also be a result of capillary condensation. Indeed, these isotherms show significant excess adsorption between the third and fourth layers. Capillary condensation is expected to be much more significant for a thicker film in the limit of $P = P_0$.

A number of recent studies found more direct evidence of capillary condensation in exfoliated graphite. A neutron-diffraction study of Ar found evidence of capillary condensed bulk crystallites once the total coverage exceeds four layers.³⁶ A recent vapor-pressure and x-ray study of multilayer Xe on exfoliated graphite found bulk Xe crystallites once a bilayer film is completed,³⁷ and a hysteresis loop extending down to bilayer surface coverage at 107 K in the adsorption-desorption cycle.

In view of these results, reports of complete wetting of Xe, Kr, CH_4 , and CO at low temperature based on vapor-pressure isotherm,^{9,10} heat-capacity,^{15,38} and NMR (Ref. 16) measurements cannot be considered as reliable.

MULTILAYER ADSORPTION ON SINGLE-CRYSTAL AND SINGLE-SURFACE GRAPHITE SUBSTRATES

There are several experiments studying multilayer film growth using single-crystal and single-surface graphite

substrate, e.g., highly oriented pyrolytic graphite (HOPG). The growth of a thick film (up to 20 layers) on a single-crystal graphite surface down to 10 and 20 K has been reported in transmission-high-energy electron-diffraction (THEED) studies, one of Xe on graphite³⁹ and the other of Ar, Kr, and Xe on graphite.⁴⁰ These films were dosed onto the graphite surface between 30 and 60 K before being cooled down to the desired temperature.

Low-temperature wetting growth was also reported in the reflection-high-energy-electron-diffraction (RHEED) studies of solid Ar, Kr, and Xe adsorbed on graphite.² In this experiment, a film of about ten statistical layers was found at low temperatures. However, a later study of CH₄ films on graphite, also using the RHEED technique,⁴¹ was interpreted to show evidence of incomplete wetting below 40 K since there were indications of bulk forming on top of 15 layers. The Xe system was repeated in the same study and found no indications of bulk up to 250 statistical layers. The film thickness beyond about four layers, however, is inferred from the exposure time of the substrate to a dosing nozzle rather than measured directly. It is not clear whether the THEED and RHEED techniques can distinguish a layered film from bulk crystallites with flat surfaces. A RHEED study of CF₄ on graphite⁴² observed an apparent wetting transition at 37 K; however, as reported above, heating-capacity,³⁴ ellipsometry,³⁵ and the current graphite fiber experiments (Fig. 8) found clear evidence of a limit of two layers below 72 K.

The most extensive studies of multilayer adsorption on graphite are those employing ellipsometry technique. For Ar and HOPG, a film with a total thickness of 11 layers is found below T_t , with distinct layer-by-layer growth for the first seven or eight layers.^{43,44} For thicknesses above the equivalent of 11 layers, bulk crystallites are found below T_t , and the limiting film thickness is found to increase to 23 layers as T is raised beyond T_t .⁴³ Similar results are found for Kr, Xe, and CH₄ on graphite, i.e., layer-by-layer growth up to seven layers just below the triple point, and a much thicker film is found just above the triple point.^{45,46} It was also reported that in the case of Kr on graphite, a film of up to hundreds of layers can be deposited onto the graphite surface, but at temperatures below T_t the thick film would subsequently break up into bulk crystallites.⁴⁵ A recent x-ray study of multilayer Xe on single-crystal graphite⁴⁷ found that the maximum thickness of Xe is limited to six layers below 55 K, seven layers at 69 K, 13 layers at 86 K, and a much thicker film (up to 24 layers) above 100 K. However, the smooth diffraction profiles for the 24-layer film are more characteristic of a uniform film with only a small number of layers. The authors suggested that the smooth profiles may be an indication that the film contained substantial rough surface and stacking faults.

One is tempted to interpret the findings of layer-by-layer growth up to seven or eight layers to be strong evidence of wetting growth below T_t . However, a recent ellipsometry experiment of N₂ on graphite is interpreted to exhibit incomplete wetting growth at temperatures between the α - β transition temperature and the triple point, in spite of the fact that layer-by-layer growth of the ad-

sorbed film is found up to ten layers.²⁵ This interpretation is prompted by the presence of β -N₂ crystallites in coexistence with the layered film.²⁵ It should also be noted that the distinct increase in the film thickness as the temperature is brought towards and exceeds the triple points found in most of the ellipsometry experiments is qualitatively consistent with our result shown in Figs. 3-6.

The "major" discrepancy between the graphite fiber experiment and the ellipsometry and the recent x-ray experiments is the limiting thickness of the adsorbed film at low temperatures. The limiting thickness on graphite fiber appears to be one or two layers thinner. It has been suggested that this discrepancy may be due to the inferior surface quality of the graphite fiber, in comparison to the HOPG and single-crystal substrates.⁴⁸ The mechanism proposed is that there are likely to be more grain boundaries for a solid film grown from an inferior surface, and these boundaries may limit the growth of thicker films. Unfortunately, it is not easy to provide a quantitative estimate of this effect. Since the single-crystal domain size on the surface of the graphite fiber has a characteristic length of 200 Å and that on HOPG is of order 10 000 Å, it is not clear to us how these length scales can be responsible for the difference in film thickness of one to two layers.

It was pointed out by Hess¹³ that very stringent requirements on temperature and hence pressure uniformity and stability must be met in order to establish and maintain true equilibrium between the adsorbed film and the surrounding vapor. This is the case because the excess substrate potential at the film surface is very small for an adsorbed film thicker than five layers. This small excess potential translates into a small depression of the coexisting vapor pressure from the saturated vapor pressure P_0 . It can be shown that in order to maintain a five-layer Ar film at equilibrium, the temperature must be uniform and stable to within 5 mK. For a film thicker than five layers, the condition becomes even more stringent. An advantage of the graphite fiber experiment is that the sample cell and the volume of the vapor phases is small (on the order of 10 cm³), and therefore much more precise temperature control is possible. The temperature of the entire sample chamber is maintained to a stability of 1 mK, and since the sample cell is made with heavy wall copper, the maximum temperature gradient that exists inside the cell is also less than 1 mK.

Another possible complication is the slow approach to equilibrium near $P = P_0$. Each of the isotherms reported here typically take 2-5 h to complete. Small doses of gas are admitted to the cell and allowed to equilibrate for about 5 min before each reading is recorded. Close to P_0 the equilibrium times can be considerably longer because a small dose of adsorbate gas can temporarily oversaturate the vapor. When this happens, the resonant frequency may drop by an amount corresponding to several layers, but always relaxes back to the equilibrium value. For a thicker film, the relaxation time can be as long as 1 h. For technical reasons, the walls of the surrounding chambers of the ellipsometry and the other single-crystal and single-surface experiments are at a much higher tem-

perature (e.g., room temperature) than the sample, and adsorbate gas is admitted continuously into the chamber in an isotherm study. Under these conditions, it is difficult to maintain the temperature of the substrate and the vapor in the immediate vicinity to a high degree (i.e., a few mK) of uniformity and stability. When P_0 is low (at low temperatures), supersaturation of the vapor over the substrate is expected, and it may be difficult to distinguish wetting film growth from epitaxial crystal growth beyond saturation.¹³

CONCLUSION

To conclude, this microbalance graphite fiber experiment found that the thickness of the adsorbed film of Ar, Kr, CH₄, and Xe on graphite is limited to a few layers at low temperature. The maximum thickness increases rapidly as T is brought toward the triple point of the adsorbate. The effective maximum film thickness at a fraction of a degree Kelvin below T_t is five to ten times smaller than that at a fraction of a degree Kelvin above T_t . Unfortunately, the ridge-trough imperfections on the surface of the graphite fiber appear to induce excess adsorption beyond what is expected for a flat substrate, and prevent a quantitative comparison of our data with the FHH equation. Since the amount of excess adsorption scales with the "expected" film thickness on a flat surface, the imperfection on the fiber surface is unlikely to alter the main, if only qualitative, conclusion of this experiment;

namely, that these four adsorption systems appear to show incomplete wetting at low temperature and wetting growth at and above the triple point of the adsorbate. The findings for these four adsorption systems are similar to those with both stronger (e.g., N₂-graphite, Ne-graphite) and weaker (e.g., O₂-graphite and C₂H₄-graphite) substrate-adsorbate interactions.² This would suggest that there is no evidence for—and there is no need to introduce the concept of—reentrant wetting for solid films on graphite at low temperatures. The results presented here appear to show that the six adsorption systems discussed in this paper (as well as a host of other adsorption systems) are consistent with the simple theoretical model for systems with strong adsorbate-substrate interaction. Whereas wetting growth is seen for liquid film at $T \geq T_t$, it is not possible at low temperature due to the structural mismatch between successive solid layers.^{3,4}

ACKNOWLEDGMENTS

We are grateful to Roger Bacon for providing the graphite fibers. We are grateful for useful conversations regarding these results with L. Bruschi, E. Cheng, J. G. Dash, M. E. Fisher, G. B. Hess, J. Krim, Y. Larher, H. Volkmann, P. Taborek, G. Torzo, and especially M. Cole. This research is supported by the National Science Foundation under Grant Nos. DMR-8718771 and DMR-9022681.

*Present address: National Institute of Standards and Technology, Division 724.03, 325 Broadway, Boulder, CO 80303.

¹R. Pandit, M. Schick, and M. Wortis, *Phys. Rev. B* **26**, 5112 (1982).

²J. L. Seguin, J. Suzanne, M. Bienfait, J. G. Dash, and J. A. Venables, *Phys. Rev. Lett.* **51**, 122 (1983); M. Bienfait, J. L. Seguin, J. Suzanne, E. Lerner, J. Krim, and J. G. Dash, *Phys. Rev. B* **29**, 983 (1984).

³D. A. Huse, *Phys. Rev. B* **29**, 6985 (1984); F. T. Gittes and M. Schick, *ibid.* **30**, 209 (1984).

⁴R. Pandit and M. E. Fisher, *Phys. Rev. Lett.* **51**, 1772 (1983).

⁵C. E. Bartosch and S. Gregory, *Phys. Rev. Lett.* **54**, 2513 (1985).

⁶J. Krim, J. P. Coulomb, and J. Bouzidi, *Phys. Rev. Lett.* **58**, 583 (1987).

⁷A. D. Migone, J. G. Dash, M. Schick, and O. E. Vilches, *Phys. Rev. B* **34**, 6322 (1986); A. D. Migone, A. Hofmann, J. G. Dash, and O. E. Vilches, *ibid.* **37**, 5440 (1988).

⁸J. Krim, J. G. Dash, and J. Suzanne, *Phys. Rev. Lett.* **52**, 640 (1984).

⁹A. Thomy and X. Duval, *J. Chim. Phys.* **67**, 286 (1970).

¹⁰B. Gilquin, D. Sc. thesis, Centre d'Etudes Nucleaires, Saclay, Report No. CEA-N-2091, 1979; F. Ser, Y. Larher, and B. Gilquin, *Mol. Phys.* **67**, 1077 (1989).

¹¹A. Terlain and Y. Larher, *Surf. Sci.* **125**, 304 (1983); C. Pierce, R. N. Nelson, J. W. Wiley, and H. Cordes, *J. Am. Chem. Soc.* **73**, 455 (1951); A. V. Kiselev and N. Y. Kovaleva, *Izv. Akad. Nauk SSSR, Otd. Khim. Nauk* **1**, 989 (1952) [*Bull. Acad. Sci., USSR, Div. J. Chem. Sci.* **6**, 955 (1959)].

¹²L. Bruschi, G. Torzo, and M. H. W. Chan, *Europhys. Lett.* **6**,

541 (1988).

¹³G. B. Hess, in *Phase Transitions in Surface Films 2*, edited by H. Taub, G. Torzo, H. J. Lauter, and S. C. Fain, Jr., (Plenum, New York, 1991), p. 357.

¹⁴Y. Larher, F. Augerand, and Y. Maurice, *J. Chem. Soc. Faraday Trans. 1*, **83**, 3355 (1987).

¹⁵M. J. Lysek, M. S. Petterson, and D. L. Goodstein, *Phys. Lett. A* **115**, 340 (1986).

¹⁶M. S. Petterson, M. J. Lysek, and D. L. Goodstein, *Surf. Sci.* **175**, 141 (1986); *Langmuir* **5**, 563 (1989).

¹⁷P. Taborek and L. Senator, *Phys. Rev. Lett.* **57**, 218 (1986).

¹⁸G. Zimmerli and M. H. W. Chan, *Phys. Rev. B* **38**, 8760 (1988).

¹⁹Fibers provided by Amoco Performance Products, Inc.

²⁰L. Bruschi and G. Torzo, in *Phase Transitions in Surface Films 2* (Ref. 13), p. 425.

²¹P. M. Morse, *Vibration and Sound* (McGraw-Hill, New York, 1948).

²²G. G. Stokes, *Mathematical and Physical Papers* (Cambridge University, London, 1922), Vol. 3, p. 38.

²³*Thermophysical Properties of Matter, Vol. II*, edited by Y. S. Touloukian, S. C. Saxena, and P. Hestermans (IFI Plenum, New York, 1975).

²⁴J. H. Dymond and E. B. Smith, *The Virial Coefficients of Pure Gases and Mixtures* (Clarendon, Oxford, 1980).

²⁵U. G. Volkmann and K. Knorr, *Phys. Rev. Lett.* **66**, 472 (1991).

²⁶J. Frenkel, *Kinetic Theory of Liquids* (Oxford, New York, 1946); G. D. Halsey, Jr., *J. Chem. Phys.* **16**, 931 (1948); T. L. Hill, *ibid.* **17**, 590 (1949).

- ²⁷I. E. Dzyoloshinskii, E. M. Lifshitz, and L. P. Pitaevskii, *Adv. Phys.* **10**, 165 (1961).
- ²⁸E. Cheng and M. W. Cole, *Phys. Rev. B* **38**, 987 (1988).
- ²⁹J. Kestin and W. Leidenfrost, *Physica* **25**, 1033 (1959).
- ³⁰L. Bruschi and G. Torzo, *Rev. Sci. Instrum.* **58**, 2181 (1987).
- ³¹P. Taborek (unpublished and private communication).
- ³²E. Cheng and M. W. Cole, *Phys. Rev. B* **41**, 9650 (1990).
- ³³M. O. Robbins, D. Andelman, and J. F. Joanny, *Phys. Rev. A* **43**, 4344 (1991).
- ³⁴Q. M. Zhang, H. K. Kim, and M. H. W. Chan, *Phys. Rev. B* **34**, 2056 (1986).
- ³⁵H. S. Nham, M. Drir, and G. B. Hess, *Phys. Rev. B* **35**, 3675 (1987).
- ³⁶J. Z. Larese, Q. M. Zhang, L. Passell, J. M. Hastings, J. R. Dennison, and H. Taub, *Phys. Rev. B* **40**, 4271 (1989); J. Z. Larese and Q. M. Zhang, *Phys. Rev. Lett.* **64**, 922 (1990).
- ³⁷K. Morishige, K. Kawamura, M. Yamamoto, and I. Ohfiyi, *Langmuir* **6**, 1417 (1990).
- ³⁸H. K. Kim, Q. M. Zhang, and M. H. W. Chan, *J. Chem. Soc., Faraday Trans. 2*, **82**, 1647 (1986).
- ³⁹G. L. Price and J. A. Venables, *Surf. Sci.* **49**, 264 (1975).
- ⁴⁰H. M. Kramer, *J. Cryst. Growth* **33**, 65 (1976).
- ⁴¹J. Krim, J. M. Gay, J. Suzanne, and E. Lerner, *J. Phys. (Paris)* **47**, 1757 (1986).
- ⁴²J. Suzanne, J. L. Seguin, M. Bienfait, and E. Lerner, *Phys. Rev. Lett.* **52**, 637 (1984).
- ⁴³H. S. Youn and G. B. Hess, *Phys. Rev. Lett.* **64**, 918 (1990).
- ⁴⁴J. W. O. Faul, U. G. Volkmann, and K. Knorr, *Surf. Sci.* **227**, 390 (1990).
- ⁴⁵H. S. Nham and G. B. Hess, *Langmuir* **5**, 575 (1989); G. B. Hess (private communication).
- ⁴⁶U. G. Volkmann and K. Knorr, *Surf. Sci.* **221**, 379 (1989).
- ⁴⁷H. Hong and R. J. Birgeneau, *Z. Phys. B* **77**, 413 (1989).
- ⁴⁸J. G. Dash, *J. Cryst. Growth* **100**, 268 (1990).